

Time-diffraction and Zitterbewegung of two-dimensional massless Dirac excitations

Elmer Cruz, Ramon Carrillo-Bastos, and Jorge Villavicencio*

Facultad de Ciencias, Universidad Autónoma de Baja California, 22800 Ensenada, Baja California, México.

(Dated: February 2, 2022)

We explore the dynamics of two-dimensional massless Dirac-fermions within a quantum shutter approach, which involves the time-evolution of an initial cut-off plane wave. We show that the probability density is governed by an interplay between *diffraction in time* and *Zitterbewegung* phenomena, typical of relativistic quantum shutter systems with nonzero mass. The *time-diffraction* appears as an oscillatory pattern in the probability density, similar to the effect predicted by Moshinsky in 1952 [Phys. Rev. **88**, 625] for Schrödinger free matter-waves. The *Zitterbewegung* manifests itself as high-frequency oscillations embedded in the time-diffraction profile. We found that these two transient effects are induced by the transverse momentum component of the incident wave, k_y , that acts as an effective mass of the system. Furthermore, this effective mass can be manipulated by tuning the incidence angle of the initial quantum state, which allows to control the frequencies of the transients. In particular, we demonstrate that near a normal incidence condition, the *Zitterbewegung* appears as a series of *quantum beats* in the probability density, with a beating frequency $2k_y v_F$, where v_F is the Fermi velocity.

PACS numbers: 73.63.Kv, 73.23.Hk, 03.65.Yz

Since the experimental discovery of graphene¹, the study of two-dimensional (2D) Dirac fermions in condensed matter physics has become of great interest both at the fundamental and applied levels². Graphene exhibits a dispersion relation with two bands touching at two singular points at the corners of the Brillouin zone. Near these Dirac points the spectrum is linear in momentum, and the electronic excitations are described by a Dirac-like equation for massless particles^{3,4}. Nevertheless, graphene is not the only condensed matter system that exhibits an effective Dirac Hamiltonian⁵, other examples include silicene⁶, germanene⁷, *Pmmn* borophene⁸, cold atoms systems⁹, and topological insulators¹⁰. These materials constitute the so call Dirac matter, and due to its relativistic Hamiltonian they have allowed probing several phenomena originally predicted by quantum electrodynamics, such as Klein tunneling^{11,12} and the *Zitterbewegung* (ZBW) effect^{13–16}, which have now become available to experimentalists^{17,18}. While the Klein tunneling occurs at equilibrium, the ZBW being an oscillation is an out of equilibrium effect, and in fact it appears as a transient phenomenon in two-dimensional Dirac systems^{14,15}. In general, transient effects^{19–21} arise from the properties of quantum waves involving either relativistic or non-relativistic equations subject to sudden changes as initial condition. The most representative transient effect is the *diffraction in time* (DIT) of free matter-waves, predicted by Moshinsky²² (1952) using a non-relativistic plane wave quantum-shutter model. A quantum-shutter setup involves a cut-off plane wave representing a matter-wave beam initially confined in a region of space ($x < 0$), stopped by an absorbing shutter at $x = 0$. After opening the shutter at $t = 0$, the free Schrödinger probability density exhibits a distinctive DIT^{22,23} oscillatory pattern, similar to the intensity profile of a light beam diffracted by a straight edge. The DIT effect was later

verified by multiple condensed matter experiments involving ultracold atoms²⁴, cold-neutrons²⁵, and atomic Bose-Einstein condensates²⁶. Also, the understanding and control of the features of DIT are of relevance, for example, in the field of atom lasers^{27–29}, which operate by extracting matter-waves from Bose-Einstein condensates. After Moshinsky's seminal paper, several theoretical works have addressed the study of transients using various initial quantum states as well as generalizations of the shutter model to explore time-dependent phenomena²⁰. However, most of these works were developed in the non-relativistic context. The first studies regarding relativistic transients involved solutions to the Klein-Gordon²² and Dirac³⁰ equations for a free massive three-dimensional particle moving in one-dimension within a plane wave quantum-shutter model. Some later works explored issues such as non-locality, forerunners, and time scales, using different types of relativistic initial conditions^{31–38}. A nice feature of these approaches is that they can describe electronic dynamics based on exact analytical solutions, which may provide a useful tool for exploring time-dependent features of 2D Dirac-matter. Moreover, although the transport effects in these 2D systems have been studied^{14,15} and the importance of transient phenomena has been stressed, until now (and up to our knowledge) the DIT for two-dimensional massless Dirac particles have not been explored.

In this work we present a new approach based on a quantum shutter model to study transient effects in 2D massless Dirac matter. By considering the Hamiltonian for graphene as typical example, we derive an exact analytical solution to explore the systems dynamics, that can be generalize to other 2D Dirac massless materials. We find that the probability density of massless Dirac-fermions exhibit two transient effects previously observed (DIT) or overlooked (ZBW) in quantum shutter approaches involving relativistic systems with non-zero

mass in vacuum. We argue that these effects are a consequence of a non-vanishing transverse momenta of the initial quantum state that acts as the mass of the system.

Cut-off plane wave model. As a prototypical example for two-dimensional Dirac matter, we describe the dynamics of low-energy electron excitations in monolayer graphene using a Dirac-like equation,

$$i\hbar\partial_t\Psi_\eta(\mathbf{r},t) = v_F\boldsymbol{\sigma}_\eta\cdot\hat{\mathbf{p}}\Psi_\eta(\mathbf{r},t), \quad (1)$$

where v_F is the Fermi velocity, $\hat{\mathbf{p}} = -i\hbar\nabla$ is the momentum operator of the charge carriers, and $\boldsymbol{\sigma}_\eta = (\eta\sigma_x, \sigma_y)$ is the vector of Pauli matrices. Following Moshinsky's²² approach, we investigate the transient behavior by taking a cut-off two-dimensional plane wave as initial condition, given by,

$$\Psi_\eta(\mathbf{r},0) = e^{i\mathbf{k}\cdot\mathbf{r}} \begin{bmatrix} 1 \\ \lambda\eta e^{i\eta\phi} \end{bmatrix} \Theta(-x), \quad (2)$$

where $\Theta(-x)$ is a Heaviside function that restricts the plane wave to the semi-infinite plane ($-\infty < x \leq 0$), modeling a perfect absorbing shutter (located at $x = 0$), that opens at $t = 0$. The wave vector is $\mathbf{k} = (k_x, k_y)$, and the incidence angle $\phi = \tan^{-1}(k_y/k_x)$. The Dirac points are labeled by $\eta = \pm 1$ (Valley K and K'), and $\lambda = \pm 1$ is for particles and holes, respectively. See Fig. 1.

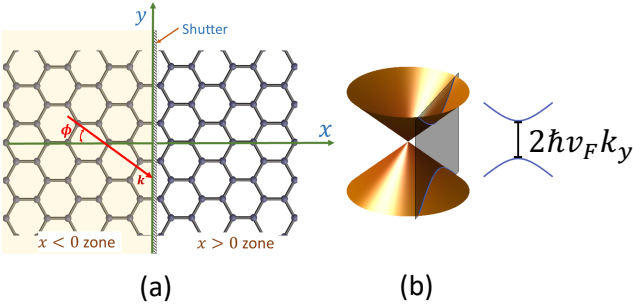


FIG. 1. (a) Quantum shutter model for electrons on the surface of a graphene monolayer. At $t = 0$ an initial state with momentum \mathbf{k} , and incidence angle ϕ , is confined in the region $x \leq 0$ by a perfect absorbent shutter located along the y -axis. (b) Dirac cone where k_y induces an energy gap that acts as an effective mass of the system.

To solve the latter system we Laplace-transform Eq. (1) with the initial condition given by Eq. (2), and obtain the following time-independent equation,

$$v_F\boldsymbol{\sigma}_\eta\cdot\nabla\tilde{\psi}_\eta(\mathbf{r},s) + s\tilde{\psi}_\eta(\mathbf{r},s) = \Psi_\eta(\mathbf{r},0). \quad (3)$$

where $\tilde{\psi}(\mathbf{r},s)$ is the Laplace transformed spinor. Here k_y is a good quantum number and thus the solution for the y coordinate will remain a plane wave. The solutions for the x coordinate must be finite in the limit $|x| \rightarrow \infty$, and

continuous at the origin ($x = 0$). This allows solving the quantum shutter problem in $(x;s)$ space for $x \geq 0$, which can be transformed back to the time-domain by explicitly computing the Bromwich inversion integrals following the procedure described in Refs. 35 and 36. Hence, the time-dependent solution can be written as

$$\Psi = \begin{bmatrix} \Phi^\uparrow(x,t) \\ \Phi^\downarrow(x,t) \end{bmatrix} e^{ik_y y} \Theta(v_F t - x), \quad (4)$$

with the spinors $\Phi^{\uparrow\downarrow}(x,t)$ given by,

$$\Phi^\uparrow(x,t) = (\alpha^+\phi_+ + \alpha^-\phi_-) - \lambda e^{i\eta\phi} J_0(\mu)/2; \quad (5)$$

$$\Phi^\downarrow(x,t) = (\beta^+\phi_+ + \beta^-\phi_-) - \eta J_0(\mu)/2. \quad (6)$$

In Eqs. (5) and (6), ϕ_\pm resemble the free-type solutions of the Klein-Gordon shutter problem²²,

$$\phi_\pm = e^{i[\pm k_x x - \lambda k v_F t]} + \frac{1}{2} J_0(\mu) - \sum_{n=0}^{\infty} (\xi/iz_\pm)^n J_n(\mu), \quad (7)$$

where $z_\pm = (\lambda k \pm k_x)/k_y$, $\xi = [(v_F t + x)/(v_F t - x)]^{1/2}$, and $J_n(\mu)$ are the Bessel functions of integer order n with argument $\mu = k_y[v_F^2 t^2 - x^2]^{1/2}$. We have also defined the coefficients,

$$\alpha^\pm = \frac{1}{2} \left(-1 \pm i\eta \frac{k_y}{k_x} \mp \frac{k}{k_x} e^{i\eta\phi} \right); \quad (8)$$

$$\beta^\pm = -\frac{\lambda}{2} \left[\pm \eta \frac{k}{k_x} + \left(\eta \pm i \frac{k_y}{k_x} \right) e^{i\eta\phi} \right]. \quad (9)$$

Equation (7) may also be written in the alternative form

$$\phi_\pm = \frac{1}{2} J_0(\mu) + \sum_{n=1}^{\infty} (-1)^n (iz_\pm/\xi)^n J_n(\mu), \quad (10)$$

useful for describing the probability density in the vicinity of $t = t_F = x/v_F$, as well as the long-time behavior of the relativistic quantum wave. We emphasize that in Ref. 22 the free Klein-Gordon solution features a DIT effect due to the electron mass, m_0 . By comparing Eq. (7) with that of Klein-Gordon's model, one may verify that the transverse momentum k_y is equivalent to $\mu_0 = m_0 c/\hbar$, which suggests that k_y serves as the mass of the system.

Our result Eq. (4) can be applied to other two-dimensional Dirac-matter systems, such as 8-*Pmmn* borophene^{39–42}, which exhibits a generalized Dirac dispersion with tilted cones. The dynamics in this type of 2D crystalline structures can be described by a massless Dirac Hamiltonian, $\hat{H} = (v_t \sigma_0 \hat{p}_y + v_x \sigma_x \hat{p}_x + v_y \sigma_y \hat{p}_y)$, where σ_i are the Pauli matrices, and \hat{p}_j the momentum operator. In the continuum model of 8-*Pmmn* borophene, the velocities⁴¹ are $v_x = 0.86v_F$, $v_y = 0.69v_F$, and $v_t = 0.32v_F$. Therefore, we can rewrite the corresponding Dirac equation $i\hbar\partial_t\psi_b(\mathbf{r},t) = \hat{H}\psi_b(\mathbf{r},t)$ by using $\psi_b(\mathbf{r},t) = \Psi_{\eta'}(\mathbf{r},t)e^{-iv_t k_y t}$ since k_y is a good quantum number, leading us to

$$i\hbar\partial_t\Psi_{\eta'}(\mathbf{r},t) = v_y\boldsymbol{\sigma}_{\eta'}\cdot\hat{\mathbf{p}}\Psi_{\eta'}(\mathbf{r},t), \quad (11)$$

where $\boldsymbol{\sigma}_{\eta'} = (\eta'\sigma_x, \sigma_y)$, and $\eta' = v_x/v_y$. The equation that describes the dynamics in borophene [Eq. (11)] is very similar to our Eq. (1) for a graphene monolayer, and hence our analytical procedure that led to Eq. (4) can be readily applied. We also argue that an alternative procedure for extending our results to other two-dimensional Dirac-matter systems, is to simply transform the Hamiltonian in $-i\hbar\partial_t\Psi'_\eta = H'\Psi'_\eta$ via a spin rotation. That is, by taking $\Psi'_\eta = \mathbf{R}\Psi_\eta$ with $H' = \mathbf{R}\boldsymbol{\sigma}_\eta \cdot \mathbf{p}\mathbf{R}^\dagger$, where $\mathbf{R} = [\mathbf{I}\cos(\theta/2) - i\boldsymbol{\sigma} \cdot \mathbf{n}\sin(\theta/2)]$ is the spin-rotation operator. As usual, \mathbf{I} is the 2×2 identity matrix, $\boldsymbol{\sigma} = (\sigma_x, \sigma_y, \sigma_z)$, and $\mathbf{n} = (n_x, n_y, n_z)$ is a unitary vector which defines the rotation axis, where θ is the rotation angle. Therefore, the transformed Hamiltonian H' can be expressed as

$$H' = v_F \cos^2(\phi/2) (\mathbf{p}_\eta \cdot \boldsymbol{\sigma}) - v_F \sin(\phi) [\mathbf{p}_\eta \times \mathbf{n}] \cdot \boldsymbol{\sigma} + v_F \sin^2(\phi/2) (\boldsymbol{\sigma} \cdot \mathbf{n}) [\mathbf{p}_\eta \cdot \mathbf{n} + i(\mathbf{p}_\eta \times \mathbf{n}) \cdot \boldsymbol{\sigma}],$$

where $\mathbf{p}_\eta = (\eta p_x, p_y)$, and by choosing $\phi = 0$, the original Hamiltonian H is recovered.

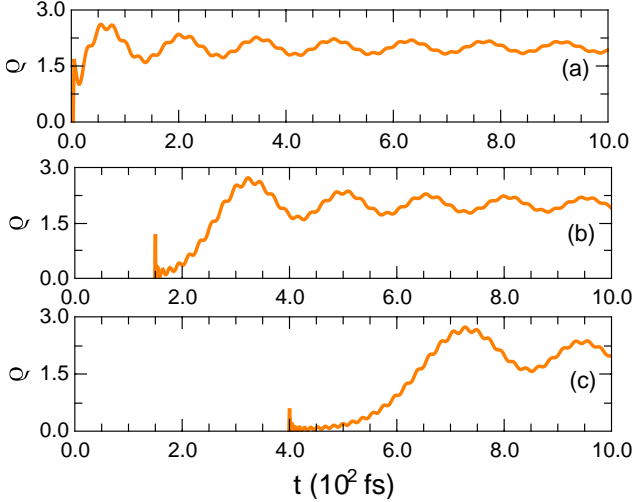


FIG. 2. Transient behavior of ρ as function of time t , with $\phi = \pi/4$, for three fixed values of position (a) $x = 5.0$ nm, (b) $x = 150.0$ nm, and (c) $x = 400.0$ nm. The probability density exhibits large oscillations similar to the DIT phenomenon typical of matter-waves. Here and in all of our calculations we set $\lambda = \eta = 1$ due to the symmetry properties of ρ , and consider an energy range $E \in [0.05, 0.2]$ eV, which is lower than the bandwidth energy (~ 3 eV) (linear momentum approximation), where we choose $E = 0.1$ eV, and $v_F = 1.0$ nm/fs.

Transient dynamics in graphene. Given the exact wavefunction in Eq. (4), we study the dynamics of quantum waves in graphene from the transient to the stationary regime. In particular, we explore the probability density, $\rho = \Psi^\dagger \Psi$, of an electron in the conduction band, localized at the K or K' valley (Dirac point). Since ρ is independent of the y coordinate, we shall study ρ as function of position x , and time t , for different values of the

incidence angle, ϕ . In Figs. 2(a)-(c) we show the time-dependence of ρ for different fixed values of position, x . We observe that ρ , from $t > t_F$ onward, grows towards a maximum value from which it oscillates until it reaches the stationary value. The large period oscillations of ρ shown in Fig. 2 are similar to the DIT phenomenon predicted in Ref. 22 and 23 for non-relativistic free matter-waves, which resembles an intensity pattern of the Fresnel diffraction of light by a semi-infinite plane. The connection with optical phenomena is further emphasized since the solutions ϕ_\pm can also be expressed in terms of Lommel functions of two variables, originally introduced in the context of optical diffraction problems⁴³. We also notice that the DIT-type profile observed in Fig. 2 exhibits embedded high-frequency oscillations. To explain the frequency content of these oscillations, we shall derive an approximate expression for ρ . We proceed by first noting that for $\phi = \pi/4$, the contributions of ϕ_- in Eqs. (5) and (6) cancel out exactly ($\alpha^- = \beta^- = 0$), allowing a simplification of Eq. (4), which now only depends on ϕ_+ . By approximating ϕ_+ using the asymptotic expansion for the Bessel functions with large values of the argument, $J_n(z) \simeq (2/\pi z)^{1/2} \cos(z - n\pi/2 - \pi/4)$, we obtain the probability density $\rho_a = \rho_{dit} + \rho_{zbw}$, with

$$\rho_{dit} \simeq 2 - \sqrt{2} \gamma t^{-1/2} \cos(k_x x - \Omega_D t - \pi/4); \quad (12)$$

$$\rho_{zbw} \simeq \left[(\sqrt{2} - 1) / (\sqrt{2} + 1) \right] z_+^{-1} \gamma t^{-1/2} \sin(k_x x - \omega t) \times \cos[(\Omega_Z t + \pi/2)/2], \quad (13)$$

where $\omega = kv_F$ is the frequency associated to the initial quantum state, and $\gamma = (8/\pi k_y v_F)^{1/2}$. In Fig. 3(a) we show that ρ_a provides a good approximation to the oscillating pattern discussed in Fig. 2(a). Also, from Eqs. (12) and (13) the dynamics of ρ_a is governed by two transient contributions, ρ_{dit} , and ρ_{zbw} . In Fig. 3(b) we show that ρ_{dit} [Eq. (12)] describes the DIT pattern, which is characterized by a frequency $\Omega_D = (k - k_y)v_F$ in the range of tens of terahertz, with a corresponding period $T_D = 2\pi\Omega_D^{-1}$ of the order of femtoseconds. In Fig. 3(c) we observe that the high-frequency secondary oscillations embedded in ρ , are a manifestation of the ZBW effect, described by the contribution ρ_{zbw} [Eq. (13)]. These oscillations are characterized by a ZBW frequency $\Omega_Z = 2k_y v_F$, in the range of hundreds of terahertz, with a period $T_Z = 2\pi\Omega_Z^{-1}$ within femtoseconds, accessible nowadays by femtosecond spectroscopy. This should be contrasted with the high-frequencies of roughly 10^{21} Hz, typical of the ZBW⁴⁴ predicted by relativistic equations for electrons in vacuum, certainly not accessible by present experimental techniques. Thus, the quantum wave dynamics involves an interplay between the DIT and ZBW phenomena. Notice also that the ZBW described by Eq. (13) exhibits a *quantum beat* effect governed by Ω_Z , that we shall later discuss in our work.

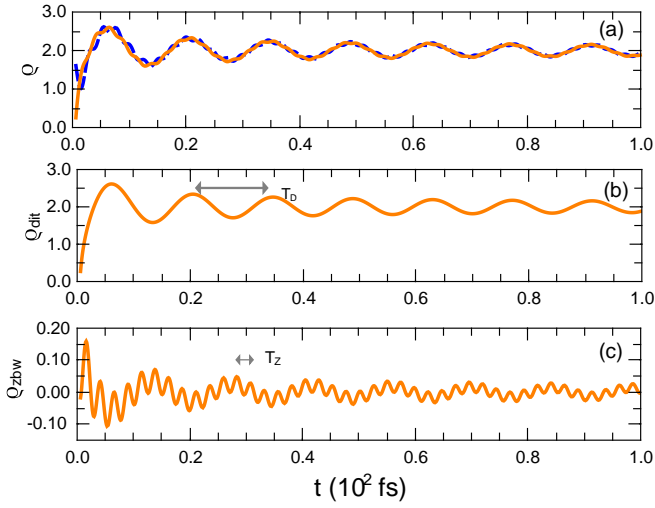


FIG. 3. (a) The DIT and ZBW phenomena in the time-evolution of the exact ρ (blue dashed line) using Eq. (4), and the asymptotic ρ_a (orange solid line) using Eqs. (12) and (13), for the case discussed in Fig. 2(a). (b) The DIT oscillations observed in (a) are described by ρ_{dif} [Eq. (12)] with a period $T_D = 141.2$ fs indicated in the plot, corresponding to a frequency $\Omega_D \sim 45.0$ THz. (c) The high-frequency oscillations embedded in the DIT pattern of case (b) are the manifestation of the ZBW effect, described by ρ_{zbw} [Eq. (13)], with a period $T_Z = 29.25$ fs, and a frequency $\Omega_Z \sim 215.0$ THz.

We stress that, although the DIT is a typical effect of quantum shutter models for systems with non-zero mass, such as those described by Klein-Gordon²² or Dirac equations³⁸, it also manifests itself in massless relativistic systems. In our relativistic case, we argue that DIT and ZBW phenomena are a result of a momentum induced effective mass due to the transverse momentum component of the incident quantum wave, $k_y = k \sin \phi$. Therefore, We expect a strong dependence of the features of quantum waves on the angle of incidence, ϕ . This is illustrated in Fig. 4(a), where ρ exhibits well defined DIT oscillations for incidences at $0 < |\phi| < \pi/2$, as shown for example in Fig. 4(c) and Fig. 4(d). Interestingly, the DIT effect is absent for the case with $\phi = 0$ (normal incidence), as shown in Figs. 4(a), and 4(b). This peculiar result involves a “massless” ($k_y = 0$) system, and is consistent with the known fact that no DIT is observed for the solution of the free quantum shutter problem for a one-dimensional wave equation²². We note that in the case discussed in Fig. 4(d), it is difficult to resolve the ZBW and DIT frequencies. To understand this behavior, in Fig 5 we compare the periods and frequencies associated with these phenomena as function of ϕ .

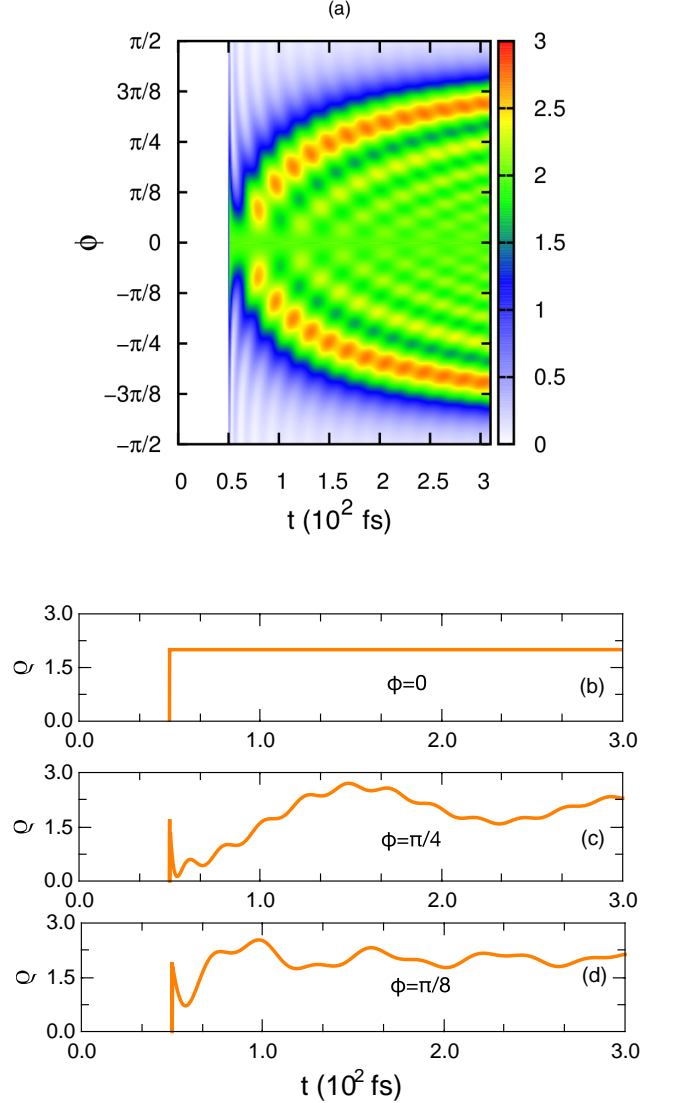


FIG. 4. (a) Surface plot of ρ as function of the incidence angle, ϕ , and time, t . The lower panel shows the probability density as function of the time t for three different values of the incidence angle (b) $\phi = 0$, (c) $\phi = \pi/4$, and (d) $\phi = \pi/8$. Here we consider a fixed position $x = 50.0$ nm, and the same parameters as in Fig. 2.

From Fig. 5 we can see that for $\phi \simeq \pi/8$, the DIT and ZBW frequencies are of the same order of magnitude *i.e.* $\Omega_Z \simeq \Omega_D$, and thus difficult to resolve, as shown in Fig. 4(d). Also, we note in Fig. 5(a) that for small values of ϕ we can easily resolve the frequencies since $\Omega_Z < \Omega_D$. We clarify that the DIT frequency, Ω_D , obtained for the case $\phi = \pi/4$, also gives a good estimate of the time-oscillation frequencies for $\phi \neq \pi/4$. As shown by our results, DIT is a robust effect observed for a wide range of values of ϕ , and characterized by transient oscillations with frequencies that are currently accessible to experiments in the field of graphene.

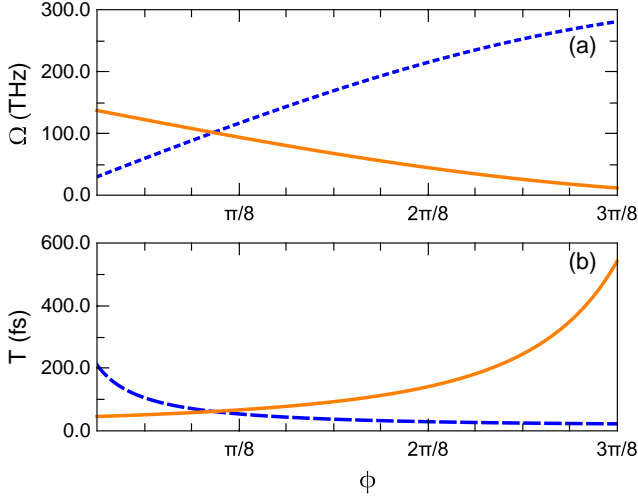


FIG. 5. (a) Plots of the periods T_D (orange solid line), and T_Z (blue dashed line) as function of ϕ . Note that for this case $\phi \simeq \pi/8$, $T_D \simeq T_Z$. (b) Plots of the frequencies Ω_D (orange solid line), and Ω_Z (blue dashed line) as function of ϕ . The frequency crossover ($\Omega_Z = \Omega_D$) occurs at $\phi = \arctan(1/\sqrt{8})$. We use the parameters of Fig. 2.

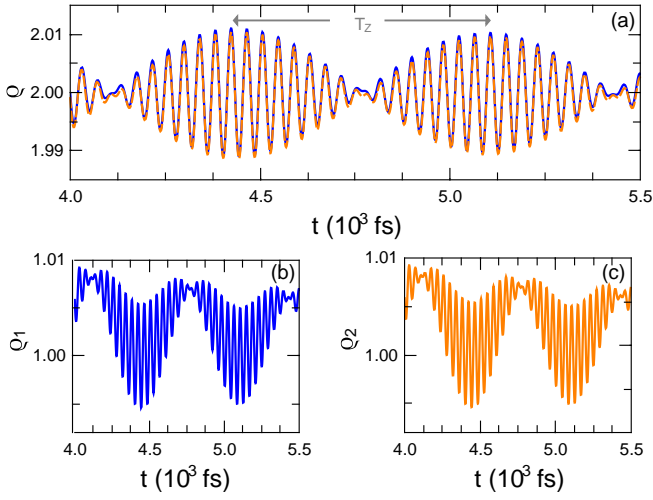


FIG. 6. (a) *Quantum beat* phenomenon in the long-time behavior of ρ using Eq. (4) (blue solid line) at fixed position $x = 50.0$ nm, for the system discussed in Fig. 2, for $\phi = \pi/100$. The frequency of the *quantum beats* is governed by the ZBW frequency, $\Omega_Z = 9.5$ THz, with a period $T_Z = 658.4$ fs, indicated in the plot. The asymptotic ρ_s (orange dashed line) is included for comparison, and almost completely overlaps with the exact solution. We also show the high-frequency beatings induced by the two asymptotic contributions (b) ρ_1 (solid blue line) and (c) ρ_2 (orange solid line).

Zitterbewegung effect. Before exploring the subject, we emphasize that ZBW is usually studied by means of the time-evolution of the expectation value of the electrons position for wave packets within Heisenberg's picture.

Moreover, it has been recognized that the ZBW effect is of a transient nature¹⁵. In this regard, we are proposing an alternative time-dependent approach to address the issue of ZBW, by exploring the transient behavior of the probability density at long-times ($t \gg t_F$). So far we have studied the interplay between DIT and ZBW phenomena, which can appear at different frequencies. We have also discussed in Fig. 5 that there is a regime of low-incidence angles, where the ZBW may be the dominant effect since $\Omega_Z < \Omega_D$. In Fig. 6 we consider the time-evolution of the probability density for the system discussed in Fig. 2, for small values of ϕ *i.e.* near the normal incidence condition ($\phi = 0$). Notice that ρ exhibits a series of *quantum beats* that modulate high-frequency oscillations, similar to the superposition phenomenon of quantum waves with different frequencies. To identify the underlying superposition that originates the *quantum beats*, we derive an asymptotic formula for the long-time behavior of ρ , for small values of ϕ . Therefore, by analyzing the asymptotic behavior of the solutions ϕ_{\pm} [Eq. (7)] with the help, as before, of the asymptotic formula for the Bessel function $J_n(z)$ for large values of the argument z , we obtain $\rho_s = \rho_1 + \rho_2$, with $\rho_1 = \rho^+$, and $\rho_2 = \cos \phi \rho^-$, with

$$\rho^{\pm} = 1 + \sqrt{2}z_{\pm}^{-1}\gamma t^{-1/2} \sin(k_x x - \omega t) \sin[(\Omega_Z t - \pi/2)/2] \pm (\gamma^2/16t)(1 + \sin \Omega_Z t). \quad (14)$$

From Eq. (14), the ZBW emerges in the probability density as a series of *quantum beats* of frequency Ω_Z , due to a superposition of sinusoidal quantum waves, with an amplitude that decays as $t^{-1/2}$. The asymptotic ρ_s fits our exact result, as shown in Fig. 6(a). Moreover, the beating frequency can be obtained by inspection of the ZBW period T_Z in Fig. 6(a) of the order of hundreds of femtoseconds, which yields frequencies in the range of tens of terahertz. The interpretation of these oscillations has been overlooked in studies addressing the problem of transients in Dirac theory^{30,38}. In our case, it is striking that an effect typical of matter-waves occurs in a system where the dynamics is associated to massless fermions.

To further explore the features of the ZBW effect in different time-regimes, we also analyze the transient behavior of the expectation value of the position operator, $\langle x \rangle$, using the exact ρ calculated from Eq. (4). Therefore, we define $\langle x \rangle$ for $x > 0$ as,

$$\langle x \rangle = \left(\int_0^{v_F t} x \rho(x, t; \phi) dx \right) / \left(\int_0^{v_F t} \rho(x, t; \phi) dx \right), \quad (15)$$

where we emphasize the explicit ϕ dependence of ρ . The integration limits are chosen to fulfill Einstein's causality *i.e.* ρ is non-zero for $x < v_F t$. We also introduce, for comparison purposes, the expectation value of position, \tilde{x} , associated to the free-propagation of massless electrons, represented by a plane wave that propagates with velocity v_F in the $\hat{k} = \mathbf{k}/k$ direction, where \mathbf{k} is the

wave vector. Thus, \tilde{x} for $x > 0$ can be expressed as,

$$\tilde{x} = \left(\int_0^{v_x t} x \rho \, dx \right) / \left(\int_0^{v_x t} \rho \, dx \right). \quad (16)$$

Since ρ is a constant over all the region $0 < x < v_F t$, and the wavefront propagation speed is $v_x = v_F \cos \phi$, by integrating Eq. (16), we obtain,

$$\tilde{x} = v_F t \cos(\phi)/2. \quad (17)$$

In Fig. 7(a) we compare the time-dependence of $\langle x \rangle$ [Eq. (15)], and \tilde{x} [Eq. (17)], for different values of ϕ .

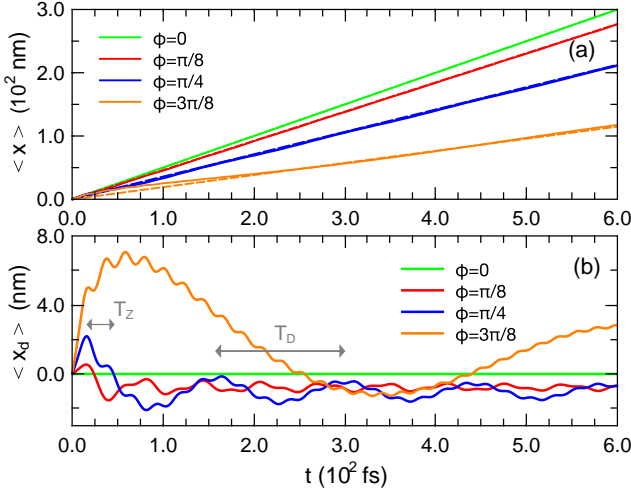


FIG. 7. (a) Time-dependence of $\langle x \rangle$ [Eq. (15)] (solid lines), and \tilde{x} [Eq. (17)] (dashed lines), for different values of the incidence angle, ϕ . The expectation value $\langle x \rangle$ slightly oscillates around the \tilde{x} , which may indicate the presence of ZBW and DIT phenomena, for different values of ϕ . (b) The average $\langle x_d \rangle$ shows an interplay between ZBW and DIT. We include in the plot the DIT and ZBW periods, $T_D = 141.2$ fs, and $T_Z = 29.5$ fs, respectively, for the particular case of $\phi = \pi/4$.

We show in Fig. 7(a) that for the case $\phi = 0$ ($k_y = 0$), the time-dependence of \tilde{x} (red dashed line), and $\langle x \rangle$ (red solid line) is characterized by a straight line, in agreement with the result reported in Ref. 18 for massless particles. We can also see in Fig. 7(a) that for values of the incidence angle in the range $0 < \phi < \pi/2$, the average position $\langle x \rangle$ (solid line) displays weak oscillations around the corresponding free-type expectation value, \tilde{x} (dashed line). We argue that \tilde{x} hinders the oscillatory behavior barely exhibited by $\langle x \rangle$, so in Fig. 7(b) we proceed to remove from $\langle x \rangle$ the contribution of \tilde{x} , by computing the difference, $\langle x_d \rangle = (\langle x \rangle - \tilde{x})$. As a result, $\langle x_d \rangle$ features a complex oscillatory pattern, reflecting the same interplay between the DIT and ZBW phenomena, that we found

by exploring the transient behavior of ρ . For example, in the case $\phi = \pi/4$ shown Fig. 7(b), $\langle x_d \rangle$ exhibits the same DIT oscillations with a period T_D , as well as the embedded secondary high-frequency ZBW oscillations with period T_Z , as discussed in Fig. 3.

Conclusions. We explore the transient dynamics of cut-off plane waves for two-dimensional massless Dirac-fermions, by deriving an exact analytical solution to a Dirac-type equation within a quantum shutter setup. Our time-dependent approach is developed for a graphene^{3,4} monolayer in the low-energy regime, and can be readily applied to other promising systems such as 8-*Pmmn* borophene^{39–42}. We find that the probability density is characterized by an interplay of two distinctive oscillatory phenomena in the time-domain: (i) a *time-diffraction* effect of frequency Ω_D , similar to the DIT²² phenomenon for Schrödinger free matter-waves; (ii) a ZBW effect which manifest itself as transient oscillations of frequency Ω_Z , embedded in the DIT-like profile. We show that these transient effects arise due to the non-zero transverse momentum of the initial quantum wave, k_y , that acts as an effective mass of the system. This acquired property of mass can be manipulated by simply tuning the incidence angle, ϕ , which allows us to adjust the frequencies Ω_D , and Ω_Z , and control to what extent the DIT or ZBW phenomena dominate the dynamics. In particular, it is shown that near a normal incidence condition, there is a time-regime where the ZBW emerges as a series of *quantum beats* in the probability density, with a beating frequency, Ω_Z , and an amplitude that decays as $t^{-1/2}$. We have found system configurations where the frequency of these transient effects are in the terahertz regime, accessible to nowadays experimentalists by using femtosecond spectroscopy. Our results may be useful in experimental setups involving the study of transient oscillations in quantum simulations like those of Ref. 18, where the terahertz regime is accessible to investigate the DIT and ZBW phenomena.

We also hope that our results may stimulate further studies on transient phenomena for cut-off quantum waves in two-dimensional materials, particularly in systems that involve different potential profiles or initial conditions, as for example by tailoring initial states as a superposition of plane waves to construct finite width wave packets.

ACKNOWLEDGEMENTS

We acknowledge useful discussions with David Ruiz-Tijerina and Mahmoud Asmar. R.C. acknowledges useful discussions with V.G. Ibarra-Sierra and J.C. Sandoval-Santana. E.C. was fully supported by Beca-PRODEP. The authors also acknowledge financial support from FC-UABC under Grant PROFOCIE 2018.

-
- * villavics@uabc.edu.mx
- ¹ K. S. Novoselov, A. K. Geim, S. V. Morozov, D. Jiang, Y. Zhang, S. V. Dubonos, I. V. Grigorieva, and A. A. Firsov, *Science* **306**, 666 (2004).
 - ² M. I. Katsnelson, *Materials Today* **10**, 20 (2007).
 - ³ A. H. Castro Neto, F. Guinea, N. M. R. Peres, K. S. Novoselov, and A. K. Geim, *Rev. Mod. Phys.* **81**, 109 (2009).
 - ⁴ K. S. Novoselov, A. K. Geim, S. V. Morozov, D. Jiang, M. I. Katsnelson, I. V. Grigorieva, S. V. Dubonos, and A. A. Firsov, *Nature* **438**, 197 (2005).
 - ⁵ J. Wang, S. Deng, Z. Liu, and Z. Liu, *National Science Review* **2**, 22 (2015), <http://oup.prod.sis.lan/nsr/article-pdf/2/1/22/8087955/nwu080.pdf>.
 - ⁶ J. Zhao, H. Liu, Z. Yu, R. Quhe, S. Zhou, Y. Wang, C. C. Liu, H. Zhong, N. Han, J. Lu, Y. Yao, and K. Wu, *Progress in Materials Science* **83**, 24 (2016).
 - ⁷ S. Cahangirov, M. Topsakal, E. Aktürk, H. Şahin, and S. Ciraci, *Phys. Rev. Lett.* **102**, 236804 (2009).
 - ⁸ X.-F. Zhou, X. Dong, A. R. Oganov, Q. Zhu, Y. Tian, and H.-T. Wang, *Phys. Rev. Lett.* **112**, 085502 (2014).
 - ⁹ S.-L. Zhu, B. Wang, and L.-M. Duan, *Phys. Rev. Lett.* **98**, 260402 (2007).
 - ¹⁰ M. Z. Hasan and C. L. Kane, *Rev. Mod. Phys.* **82**, 3045 (2010).
 - ¹¹ M. Katsnelson, K. Novoselov, and A. Geim, *Nature physics* **2**, 620 (2006).
 - ¹² S.-H. Zhang and W. Yang, *Phys. Rev. B* **97**, 235440 (2018).
 - ¹³ M. I. Katsnelson, *The European Physical Journal B - Condensed Matter and Complex Systems* **51**, 157 (2006).
 - ¹⁴ G. Maksimova, V. Y. Demikhovskii, and E. Frolova, *Physical Review B* **78**, 235321 (2008).
 - ¹⁵ T. M. Rusin and W. Zawadzki, *Phys. Rev. B* **76**, 195439 (2007).
 - ¹⁶ V. Krueckl and T. Kramer, *New Journal of Physics* **11**, 093010 (2009).
 - ¹⁷ N. Stander, B. Huard, and D. Goldhaber-Gordon, *Phys. Rev. Lett.* **102**, 026807 (2009).
 - ¹⁸ R. Gerritsma, G. Kirchmair, F. Zähringer, E. Solano, R. Blatt, and C. F. Roos, *Nature* **463**, 68 EP (2010).
 - ¹⁹ M. Kleber, *Phys. Rep.* **236**, 331 (1994).
 - ²⁰ A. D. Campo, G. García-Calderón, and J. G. Muga, *Phys. Rep.* **476**, 1 (2009).
 - ²¹ M. Razavy, *Quantum Theory Of Tunneling (2nd Edition)* (World Scientific Publishing Company, 2013).
 - ²² M. Moshinsky, *Phys. Rev.* **88**, 625 (1952).
 - ²³ M. Moshinsky, *American Journal of Physics* **44**, 1037 (1976), <https://doi.org/10.1119/1.10581>.
 - ²⁴ P. Szriftgiser, D. Guéry-Odelin, M. Arndt, and J. Dalibard, *Phys. Rev. Lett.* **77**, 4 (1996).
 - ²⁵ T. Hils, J. Felber, R. Gähler, W. Gläser, R. Golub, K. Habicht, and P. Wille, *Phys. Rev. A* **58**, 4784 (1998).
 - ²⁶ Y. Colombe, B. Mercier, H. Perrin, and V. Lorent, *Phys. Rev. A* **72**, 061601 (2005).
 - ²⁷ E. W. Hagley, L. Deng, M. Kozuma, J. Wen, K. Helmerston, S. L. Rolston, and W. D. Phillips, *Science* **283**, 1706 (1999).
 - ²⁸ M. Trippenbach, Y. B. Band, M. Edwards, M. Doery, P. S. Julienne, E. W. Hagley, L. Deng, M. Kozuma, K. Helmerston, S. L. Rolston, and W. D. Phillips, *Journal of Physics B: Atomic, Molecular and Optical Physics* **33**, 47 (2000).
 - ²⁹ A. del Campo, J. G. Muga, and M. Moshinsky, *Journal of Physics B-atomic Molecular and Optical Physics* **40**, 975 (2007).
 - ³⁰ M. Moshinsky, *Rev. Mex. Fis.* **1**, 151 (1952).
 - ³¹ M. Büttiker and H. Thomas, *Superlattices and Microstructures* **23**, 781 (1998).
 - ³² J. G. Muga and M. Büttiker, *Phys. Rev. A* **62**, 023808 (2000).
 - ³³ F. Delgado, J. G. Muga, A. Ruschhaupt, G. García-Calderón, and J. Villavicencio, *Physical Review A* **68**, 32101 (2003).
 - ³⁴ J. Deutch and F. Low, *Annals of Physics* **228**, 184 (1993).
 - ³⁵ G. García-Calderón, A. Rubio, and J. Villavicencio, *Phys. Rev. A* **59**, 1758 (1999).
 - ³⁶ J. Villavicencio, *Journal of Physics A: Mathematical and General* **33**, 6061 (2000).
 - ³⁷ G. Kälbermann, *Journal of Physics A: Mathematical and General* **34**, 6465 (2001).
 - ³⁸ S. Godoy and K. Villa, *Journal of Modern Physics* **07**, 1181 (2016).
 - ³⁹ A. Lopez-Bezanilla and P. B. Littlewood, *Phys. Rev. B* **93**, 241405 (2016).
 - ⁴⁰ B. Peng, H. Zhang, H. Shao, Y. Xu, R. Zhang, and H. Zhu, *J. Mater. Chem. C* **4**, 3592 (2016).
 - ⁴¹ A. D. Zabolotskiy and Y. E. Lozovik, *Phys. Rev. B* **94**, 165403 (2016).
 - ⁴² S. Verma, A. Mawrie, and T. K. Ghosh, *Phys. Rev. B* **96**, 155418 (2017).
 - ⁴³ G. Watson, *A Treatise of the Theory of Bessel Functions* (Cambridge Mathematical Library, 1996).
 - ⁴⁴ A. O. Barut and A. J. Bracken, *Phys. Rev. D* **23**, 2454 (1981).